

Coupling of surface waves in highly defined one-dimensional porous silicon photonic crystals for gas sensing applications

Emiliano Descrovi^{a)}*Dipartimento di Fisica, Politecnico di Torino, C.so Duca degli Abruzzi 24, 10129 Torino, Italy*

Francesca Frascella, Beniamino Sciacca, and Francesco Geobaldo

Dipartimento di Scienza dei Materiali e Ingegneria Chimica, Politecnico di Torino, C.so Duca degli Abruzzi 24, 10129 Torino, Italy

Lorenzo Dominici and Francesco Michelotti

Dipartimento di Energetica, SAPIENZA Università di Roma, Via A. Scarpa 16, 00161 Roma, Italy

(Received 27 July 2007; accepted 21 November 2007; published online 13 December 2007)

We describe the use of one-dimensional porous silicon (*p*-Si) photonic crystals for guiding TE-polarized surface electromagnetic waves (SEWs). Although bulk and interface roughnesses might deteriorate the optical response of photonic structures, we observed reflection spectra presenting narrow (≤ 6 nm) reflectivity anomalies associated with SEWs. In analogy with surface plasmons, SEWs are strongly sensitive to surface modifications. As a proof of principle for a sensor, we provide a direct real-time monitoring of the reversible interactions of organic vapors with the *p*-Si multilayer. We highlight the higher sensitivity of the SEW-based detection scheme as compared to a method exploiting perturbations of waveguide modes. © 2007 American Institute of Physics. [DOI: 10.1063/1.2824387]

In the past years, surface plasmon resonance¹ (SPR) phenomena reached wide popularity in a number of different domains such as nonlinear optics,² near-field microscopy/spectroscopy,^{3,4} and gas sensing.⁵ This large interest is mainly connected to two important features of surface plasmon polaritons (SPPs): their strong electromagnetic field enhancement and their sensitivity upon changes of the refractive index at metal/dielectric interfaces. Unfortunately, the large absorption at optical frequencies in metals results in a dumping of plasmons and a broadening of the SPR profile until several tens of nanometers.

Alternatively, if dielectric materials are used, the condition for the existence of surface waves can be accomplished by employing specifically engineered artificial media such as photonic crystals. In fact, it was shown that TE-polarized surface electromagnetic waves (SEWs) satisfy Maxwell's equations at the boundaries of truncated one-dimensional (1D) photonic crystals.^{6,7} In analogy with SPPs, SEWs feature quite large field amplitudes at interfaces. In addition, the field enhancement factor as well as the spectral position of SEWs can be tuned by a proper design of the structure layers.⁸ Dielectric materials are characterized by much lower absorption coefficients than metals, therefore Wood anomalies⁹ associated with SEWs appear much narrower.

In this work, we consider coupling to SEWs in porous silicon (*p*-Si) 1D photonic crystals. We demonstrate that SEWs are connected to remarkably narrow Wood's anomalies which allow us to perform real-time gas detection with high sensitivity.

p-Si is a suitable candidate for the fabrication of photonic crystals because of the large refractive index contrast it can exhibit. Moreover, its large specific surface makes sensing applications particularly attractive.¹⁰ As a drawback, the high roughness of interfaces and bulk material

can deteriorate the optical response of the whole photonic structure.

Here, we consider a 25 period stack of high (*H*) and low (*L*) refractive index layers characterized by the following thicknesses and porosities: $d_H=215$ nm, $p_H=49\%$ and $d_L=240$ nm, $p_L=58\%$, respectively. *p*-Si 1D photonic crystals were electrochemically etched starting from highly B-doped *p*⁺-type Si(100), 7.13 m Ω cm. The etching process was performed at -25 °C (Ref. 11) in a solution composed by HF(35%):H₂O:C₂H₅OH in volume ratio of 18:18:64. The etching rate and porosity were calibrated as a function of the anodization current density by means of UV-vis-NIR reflectivity performed on single porous layers at 12° incidence angle in the range of 200–3200 nm. Such a wide spectral range allowed us to retrieve satisfactory calibration parameters and also to estimate the full refractive index dispersion. At $\lambda=1530$ nm, we obtained the following $n_H=2.15$ and $n_L=1.89$.

The calculated band structure of an infinite stack of *H-L* bilayers is presented in Fig. 1. Dark and white regions indicate allowed and forbidden bands, respectively. The β wave-numbers on the abscissa axis represents the wave propagation constant in a direction parallel to the planar surfaces of the multilayer.

The dispersion curves of guided modes in the allowed regions of the truncated 25 period structure are also shown as tiny, narrow white lines. Calculations were carried out by means of the translation operator method described by Yeh *et al.*¹² Since surface modes are dumped in both homogeneous (air) and structured (photonic crystal) media, their corresponding Bloch wavevectors are complex. As a consequence, SEW dispersion curves lie inside forbidden bands.

Experimental measurements of the dispersion curves of SEWs in the 1450–1590 nm range were performed with the help of an Otto spectroscopic single prism coupling setup. A collimated and TE-polarized beam extracted and expanded

^{a)}Electronic mail: emiliano.descrovi@polito.it

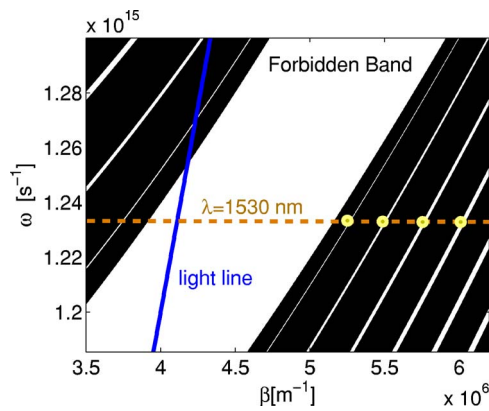


FIG. 1. (Color online) Band structure and guided modes supported by a 25 period *H-L p-Si* bilayer. The considered wavelength interval ranges from 1450 to 1590 nm. Solid circles indicate the position of some of the guided modes sustained by the structure at $\lambda = 1530$ nm.

from an external cavity tunable diode laser source (Nettest, Tunics-Plus) is focused on the sample by means of a low numerical aperture lens ($f=250$ mm) through the input facet of a 45° glass coupling prism ($n_{\text{prism}}=1.66$). The prism is pressed on the photonic crystal front face by means of a screw. The air gap between prism and sample can be coarsely adjusted by varying the pushing force. The multilayer was designed in such a way that a forbidden band is almost superimposed to the light line associated with the prism air interface (see Fig. 1). For this reason, we expect to couple SEW at an illumination angle slightly just larger than the critical angle. As it is well known, the air gap between the guiding structure and the prism is a critical issue in the Otto

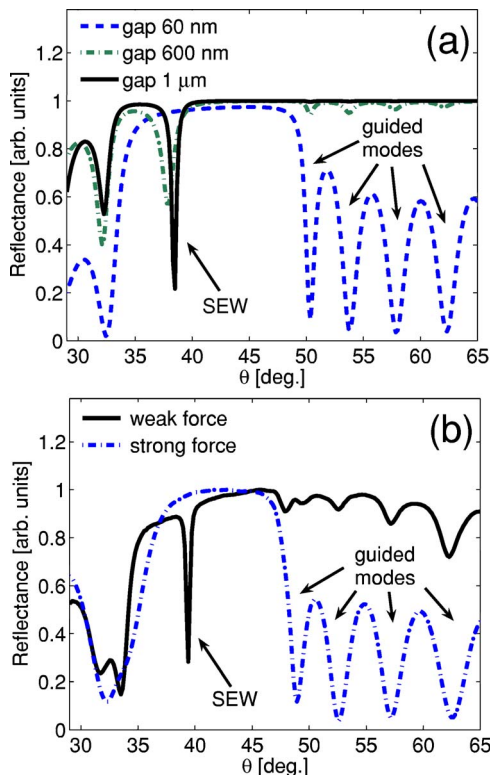


FIG. 2. (Color online) Calculated normalized reflectance as a function of the incident angle θ for three different values of the air gap between coupling prism and multilayer. (b) Measured normalized reflectance in the Otto setup for two different values of the force pressing the multilayer against the prism. Incident wavelength is $\lambda = 1530$ nm.

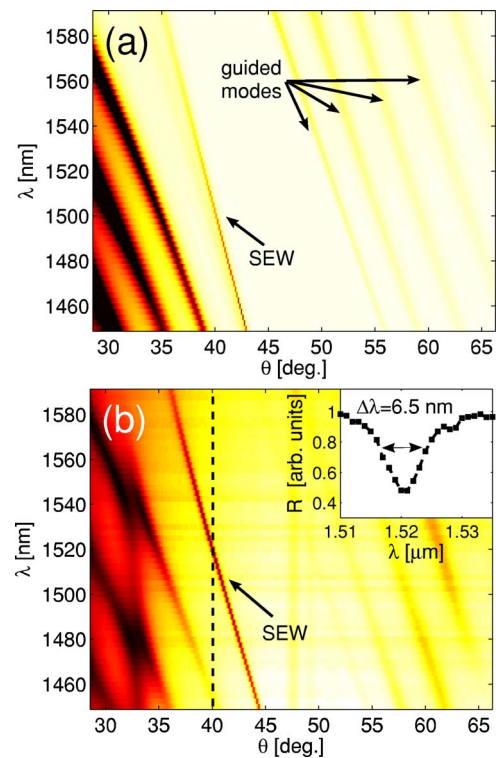


FIG. 3. (Color online) (a) Calculated and (b) measured spectroscopic-angular reflectance maps of *p-Si* multilayer. Wood anomaly associated with SEW has a FWHM=6.5 nm at $\theta=40^\circ$ (see inset). Dark color means low reflectivity.

setup. The influence of such a gap on the SEW coupling is considered both theoretically and experimentally in Fig. 2.

As predicted by theory¹³ and confirmed by our rigorous calculations based on Rayleigh wave expansion, when the air gap is below a certain threshold value, the excited modes get leaky and small modulations of reflectance due to mode coupling can be observed. On the other hand, if the gap becomes too wide, the coupling strength dramatically decreases, although the mode dips become narrower. At small gaps (corresponding to a strong mechanical forces pushing on the sample), modes having large propagation constants $\beta = 2\pi n_{\text{prism}} \sin \theta / \lambda$ are preferentially coupled (dashed lines). In this situation, we recognize some of the guided modes shown in Fig. 1 but clearly no power is transferred to the surface mode. As the pushing force decreases, the air gap increases and a sharp dip appears within the forbidden band (solid line), while the coupling strength for guided modes becomes negligible.

Once the optimum coupling was found, we were able to map the multilayer reflectance over rather wide spectral and angular ranges, thus revealing the actual dispersion curves of coupled modes. Measured full spectroscopic-angular maps and calculations are both shown in Fig. 3. An excellent agreement between experiment and calculations was obtained. In particular, we underline the narrowness of the dip [full width at half maximum (FWHM)=6.5 nm] associated with SEW found at an incidence angle $\theta=40^\circ$ and stress out that dips related to SEW become even narrower with increasing β . This result, also confirmed by calculations, is a direct consequence of the use of Otto coupling configuration. The well-defined features observed experimentally demonstrate that the roughness level of the fabricated multilayer is low

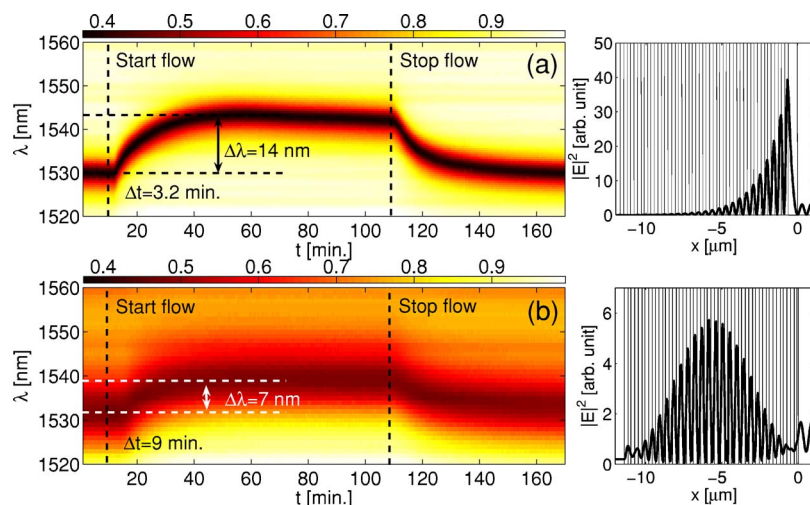


FIG. 4. (Color online) Real-time measurement of the reflected light in the spectral range $\lambda \in [1520, 1560]$ nm from the *p*-Si multilayer exposed at ethanol vapor during a limited time interval. (a) SEW at $\theta=37.60^\circ$ and (b) guided mode at $\theta=47.49^\circ$. Field intensity distributions of the selected modes are shown beside.

enough to preserve an excellent optical response of the whole structure.

p-Si Bragg mirrors were proposed in the recent past for gas sensing.^{14–16} A very recent work reported on the shift of the resonance on *p*-Si multilayers after irreversible chemical functionalization by amino groups.¹⁷ We show here the high sensitivity of our *p*-Si SEW device as vapor sensor and compare it to that resulting from the perturbation of a waveguide mode. We coupled either the SEW ($\theta=37.60^\circ$) or the first guided mode ($\theta=47.49^\circ$) placed beyond the forbidden band at larger β [see Fig. 3(b)]. In each case, we refined the width of the prism-sample gap and obtained comparable depths of the resonances, in order to set for comparison between the two sensing responsivities. In Fig. 4, we show the real-time measurement of the reflected signal in the spectral range $\lambda \in [1520, 1560]$ nm, both for SEW (top) and guided mode (bottom), as a flow of ethanol vapor coming from a saturated chamber penetrates the air gap between the multilayer and the prism. In both cases, the ethanol flow starts at $t \approx 9$ min, is maintained constant for a limited time interval and then stopped at $t \approx 107$ min. The signals were detected with a 27.2 s sampling rate, which is fast enough to avoid any distortion of the spectrum shape during each wavelength sweep.

Results presented in Fig. 4 put into evidence several improved features of the SEW-based sensing with respect to the mode-based one: (1) a larger shift of the resonance wavelength ($\Delta\lambda=14$ nm for SEW and $\Delta\lambda=7$ nm for the guided mode); (2) a shorter delay (3.2 min for SEW and 9 min for the guided mode) starting from the initial vapor in-flow time; and (3) the dip is much narrower in SEW as compared to the guided mode. This last feature produces a much shorter rise time in a practical sensing configuration where the response is detected at the fixed initial resonance wavelength.

As a conclusion, in this work, we presented a detailed experimental characterization of electromagnetic surface waves coupled on *p*-Si multilayers. Furthermore, we demonstrated that SEW-based detection can be fruitfully employed in real-time monitoring of physical/chemical processes taking place at the multilayer-free surface. In particular, we underlined the higher sensitivity of such a technique in the specific case of ethanol vapor sensing as compared to a planar waveguide mode perturbation method.

¹H. Raether, *Surface Plasmons on Smooth and Rough Surfaces and on Gratings*, Tracts in Modern Physics Vol. 111 (Springer, Berlin, Heidelberg, 1988), Chap. 1.

²J. C. Quail, J. G. Rako, H. J. Simon, and R. T. Deck, *Phys. Rev. Lett.* **50**, 1987 (1983).

³F. Keilmann, *J. Microsc.* **194**, 567 (1999).

⁴A. Bouhelier, M. R. Beversluis, and L. Novotny, *Ultramicroscopy* **100**, 413 (2003).

⁵M. G. Manera, C. de Julian Fernández, G. Maggioni, G. Mattei, S. Carturan, A. Quaranta, G. Della Mea, R. Rella, L. Vasanelli, and P. Mazzoldi, *Sens. Actuators B* **120**, 712 (2007).

⁶P. Yeh and A. Yariv, *Appl. Phys. Lett.* **32**, 104 (1978).

⁷W. M. Robertson and S. May, *Appl. Phys. Lett.* **74**, 1800 (1999).

⁸M. Shinn and W. M. Robertson, *Sens. Actuators B* **105**, 360 (2005).

⁹W. Wood, *Philos. Mag.* **4**, 396 (1902).

¹⁰J. Volk, T. Le Grand, I. Bársony, J. Gombkő, and J. J. Ramsden, *J. Phys. D* **38**, 1313 (2005).

¹¹F. Geobaldo, P. Rivolo, S. Borini, L. Boarino, G. Amato, M. Chiesa, and E. Garrone, *J. Phys. Chem. B* **108**, 18306 (2004).

¹²P. Yeh, A. Yariv, and C.-S. Hong, *J. Opt. Soc. Am.* **67**, 423 (1977).

¹³R. Ulrich, *J. Opt. Soc. Am.* **60**, 1337 (1970).

¹⁴P. A. Snow, E. K. Squire, P. St. J. Russell, and L. T. Canham, *J. Appl. Phys.* **86**, 1781 (1999).

¹⁵P. Allcock and P. A. Snow, *J. Appl. Phys.* **90**, 5052 (2001).

¹⁶P. J. Reece, G. Lérondel, J. Mulders, W. H. Zheng, and M. Gal, *Phys. Status Solidi A* **197**, 321 (2003).

¹⁷E. Guillermain, V. Lysenko, R. Orobchouk, T. Benyattou, S. Roux, A. Pillonnet, and P. Perriat, *Appl. Phys. Lett.* **90**, 241116 (2007).